Title

Multiscale biomechanical responses of adapted bone–periodontal ligament–tooth fibrous joints

Authors

Jang, Andrew T
Merkle, Arno P
Fahey, Kevin P
et al.

Publication Date

2015-12-01

DOI

10.1016/j.bone.2015.07.004

Peer reviewed

HHS Public Access

Author manuscript

Bone. Author manuscript; available in PMC 2016 December 01.

Published in final edited form as:

Bone. 2015 December ; 81: 196–207. doi:10.1016/j.bone.2015.07.004.

Multiscale biomechanical responses of adapted bone-periodontal ligament-tooth fibrous joints

Andrew T. Jang[+], **Arno Merkle**[*], **Kevin Fahey**[*], **Stuart A. Gansky**[#], and **Sunita P. Ho**[+,α]

[+]Division of Biomaterials and Bioengineering, Department of Preventive and Restorative Dental Sciences, University of California San Francisco, CA 94143

[#]Division of Oral Epidemiology & Dental Public Health, Department of Preventive and Restorative Dental Sciences, University of California San Francisco, CA 94143

[*]Carl Zeiss X-ray Microscopy, Inc., 4385 Hopyard Road, Suite 100, Pleasanton, CA 94588

Abstract

Reduced functional loads cause adaptations in organs. In this study, temporal adaptations of bone-ligament-tooth fibrous joints to reduced functional loads were mapped using a holistic approach. Systematic studies were performed to evaluate organ-level and tissue-level adaptations in specimens harvested periodically from rats given powder food for 6 months (N = 60 over 8,12,16,20, and 24 weeks). Bone-periodontal ligament (PDL)-tooth fibrous joint adaptation was evaluated by comparing changes in joint stiffness with changes in functional space between the tooth and alveolar bony socket. Adaptations in tissues included mapping changes in the PDL and bone architecture as observed from collagen birefringence, bone hardness and volume fraction in rats fed soft foods (soft diet, SD) compared to those fed hard pellets as a routine diet (hard diet, HD). *In situ* biomechanical testing on harvested fibrous joints revealed increased stiffness in SD groups (SD:239-605 N/mm) ($p<0.05$) at 8 and 12 weeks. Increased joint stiffness in early development phase was due to decreased functional space (at 8wks change in functional space was −33 μm, at 12wks change in functional space was −30 μm) and shifts in tissue quality as highlighted by birefringence, architecture and hardness. These physical changes were not observed in joints that were well into function, that is, in rodents older than 12 weeks of age. Significant adaptations in older groups were highlighted by shifts in bone growth (bone volume fraction 24wks: Δ-0.06) and bone hardness (8wks: Δ−0.04 GPa, 16 wks: Δ−0.07 GPa, 24wks: Δ−0.06 GPa). The response rate (N/s) of joints to mechanical loads decreased in SD groups. Results from the study showed that joint adaptation depended on age. The initial form-related adaptation (observed change in functional space) can challenge strain-adaptive nature of tissues to meet functional demands with increasing age into adulthood. The coupled effect between functional space in the bone-PDLtooth complex and strain-adaptive nature of tissues is necessary to accommodate functional demands, and is temporally sensitive despite joint malfunction. From an

[α]To whom correspondence should be addressed: Sunita P. Ho, Ph.D., Division of Biomaterials and Bioengineering, Department of Preventive and Restorative Dental Sciences, 707 Parnassus Avenue, University of California San Francisco, CA 94143-0758, sunita.ho@ucsf.edu, Phone: 415-514-2818.

applied science perspective, we propose that adaptations are registered as functional history in tissues and joints.

1. INTRODUCTION

Functional loads arise from every day activities and are the primary environmental factors responsible for guiding tissue and organ development and growth [1,2]. From a developmental standpoint, stiffness gradients due to passive stretch in matrices are thought to play a role in cell polarity, differentiation, organization, migration, and contribute to the synthesis and turnover of organic and inorganic constituents [3]. Subsequently, during growth, tissue maturation through increasing number of crosslinks in organic matrices and phase changes in mineral [4] occur based on functional cues throughout the lifespan of an organism [1].

In a bone-periodontal ligament (PDL)-tooth fibrous joint, the primary functional loads are enabled by the muscles of mastication, including the masseter, temporalis, medial pterygoid, and the upper/lower lateral pterygoid [5,6]. Magnitudes and frequencies of functional loads are dependent on many intrinsic and extrinsic factors [7], including muscle efficiency (e.g. higher in men vs. women, higher in younger vs. older [8–10]), diet hardness (e.g. softer foods and/or liquid diet vs. harder foods [11,12]), and other forms of behavioral loads (e.g. nail biting, tongue trusting, jaw clenching, bruxism [13,14]). As a result, functional loads within the oral cavity are categorized as physiologic (e.g. food chewing), pathogenic (e.g. bruxism), and therapeutic (e.g. orthodontic loads). Hence, it is conceivable that a change in magnitude of functional loads due to one or more of these factors can change the axial and lateral loads on a tooth and its relative position within the alveolar socket. In this study, functional adaptation by evaluating overall changes in biomechanics of a fibrous joint and adaptation of the respective tissues the makeup the joint were investigated by modulating chewing forces and frequencies through hardness of food given to rats.

Functional (i.e. overload, disuse, and directional load) adaptations in bone, cementum, and the PDL are often evaluated systematically using small-scale animal models, such as rodents. Studies focusing on muscle activity have noted a decrease in muscle contraction and an increase in contraction rate with a decrease in magnitude and an increase in loading frequency when hard pellet diet (HD) normally given to rats is replaced with either liquid, pudding, or powder soft diets (SD) [15,16]. Studies leveraging the load-mediated response have mapped changes in mass of alveolar bone [17,18], bone architecture [19], and PDL orientation and turnover rates. A previous study from our laboratory reported changes in hardness of alveolar bone and cementum, and mineral profile changes across the bone-PDL-cementum complex harvested from rats subjected to SD [20].

Considering the fibrous, hygroscopic, vascular, and innervated nature of the ligament between the tooth and the vascularized alveolar socket, the bone-PDL-cementum complex contains biophysical and biochemically graded fibrous PDL-bone and PDL-cementum entheses [21]. Early investigators isolated and performed biomechanical studies on transverse sectioned blocks of the bone-PDL-tooth complex and focused on the PDL's intrusive, extrusive and related viscoelastic/viscoplastic characteristics [22–26].

Subsequently, by using an *in situ* mechanical loading device coupled to an x-ray microscope, biomechanical studies on intact bone-PDL-tooth fibrous joints, and geometric relationship of tooth with the alveolar socket in humans [27] and other mammalian models under normal [28–30] and diseased conditions [31] were performed.

In this study, following reduced chewing forces on bone-PDL-tooth complexes of rats for a period of 20 weeks (24 weeks total age), the questions that were asked included: 1) is there a shift in biomechanics of fibrous complex exposed to reduced functional loads? 2) Do adaptive properties of tissues, i.e. physicochemical properties of bone, cementum, and periodontal ligament in reduced-function and normal-function groups converge to similar patterns with the age of the mammal? 3) What is the clinical significance in adaptive properties (physicochemical) of softer and harder tissues within the joint under prolonged reduced function? These questions were explored by designing experiments to identify shifts in stiffness of fibrous joints from HD and SD groups and correlating the shifts to tissue-level adaptations in respective groups. Hence the objective of the study was to use a holistic approach (as opposed to commonly adopted reductionist approach), in that, insights into tissue adaptations in rats aged 6 to 24 weeks were evaluated and discussed within the context of overall biomechanics of intact joints. Results demonstrated an altered biomechanical response of the fibrous joint through identifiable changes in: 1) joint reactionary response to *in situ* loading as seen by load-displacement and load-time relationships, and by comparing these readings to 2) changes in organization and structure of adapted hard/soft tissues and 3) bulk material properties of hard tissues.

2. MATERIALS AND METHODS

2.1. Reduced functional load animal model

All experimental protocols were compliant and followed the guidelines of the Institutional Animal Care and Use Committee (IACUC) [20]. Sprague Dawley male rats (N = 60; Charles River Laboratories, Inc., Willmington, MA) at 4 weeks of age were divided into 2 groups and fed one of two nutritionally equivalent foods, which differed only in hardness, hard pellet food (Hard Diet = HD; N = 30) or soft powder chow (Soft Diet = SD; N = 30) (PicoLab 5058, LabDiet, Deans Animal Feeds, Redwood City, CA, USA).

To measure the effects of load-mediated changes due to food hardness across age groups, separate animals groups were grown to 8, 12, 16, and 24 weeks. Mandibles were harvested from sacrificed animals at each time point and separated into right and left hemimandibles (Fig. 1). Right hemimandibles were used to perform biomechanical testing using an *in situ* loading device coupled to a micro X-ray computed tomography/microscopy unit (Micro XCT-200, Carl Zeiss, Pleasanton, CA) (Fig. 1a and b). Specimens were stored in a tris-phosphate buffer solution supplemented with 50 μg/mL of penicillin and streptomycin [32]. Left hemimandibles were processed for histology.

2.2. Biomechanical testing and *in situ* imaging of functional-space in intact fibrous joints

The harvested hemimandibles were prepared for *in situ* biomechanical testing as described previously [28,29]. Prepared specimens were loaded *in situ* (MT500CT, Deben UK Ltd,

Suffolk, UK) to several displacement rates (0.2, 0.5, 1.0, 1.5, 2.0 mm/min) and peak loads (5N, 6N, 8N, 10N, 15N) within the detectable ranges of the mechanical testing device (Fig. 2). The load cell outputs of time, reactionary response to load, and displacement (Fig. 1d) were further processed to describe the biomechanical response of the dentoalveolar complex (stiffness and loading rate response) [28,29]. Joint stiffness (N/mm) was calculated by approximating the final 30% of the load vs. displacement graph [29,33,34] with a linear regression model (Fig. 1c). Reactionary response of the joint to loads was calculated by evaluating load rate (N/s) from load vs. time gradient similar to stiffness. Relationships between parameters were evaluated statistically across age and diet groups and across the gradient within the specimens using a mixed effects regression model with random specimen effects. To highlight the multivariable effects of our data, 3D surface plots relating joint stiffness against a two dimensional axis (age and displacement, age and peak load) were generated using a custom MATLAB code (MATAB, Mathworks, Natick, MA).

Specimens used for biomechanical testing were also imaged using X-ray microscopy (XRM) (Micro XCT-200, Xradia, Pleasanton, CA) to identify structural changes within the dentoalveolar complex. A virtual sagittal plane bisecting the distal and mesial lingual roots of the 2nd molar was selected from tomograms taken at no load to evaluate changes in functional PDL-space. Functional PDL-spaces were measured between tooth and bone specifically in the interradicular region and the data was compared within and across HD and SD groups.

2.3. Hardness of bone, cementum and dentin

Specimens were cut orthogonally to the occlusal plane (sagittal) of the molars into two halves and embedded in epoxy. The exposed surface containing the bone-PDL-tooth complex was polished using a series of fine diamond suspension slurries (Buehler Ltd., Lake Bluff, IL) [35]. Microindentation was performed on the secondary cementum (located at the apical 1/3 of the root) of the tooth, interradicular bone, and interdental bone of the alveolar complex using a Knoop indenter [35]. Rows of microindents (10 seconds, 20 gf, dry conditions) were arranged according to ASTM E384-99 [36].

3.3. 2.4. Collagen fiber birefringence and root-PDL directionality in adapted complexes

Histology sections containing an intact distal root from the 2nd molar were selected for PSR staining (n=3 at all time points and diet groups) [31]. Stained slides were analyzed using a directionality function of Fiji (Jean-Yves Tinevez, [37]) to compute PDL directionality. PDL directionality measurements of the mid-root were taken on the mesial and distal sides and were analyzed for age and diet trends. Quantification of orientation through birefringence was performed by rotating the specimen stage until the region of interest illustrated maximum birefringence. Average intensities over tissue area were calculated in the following regions: interradicular bone (IR-B), interradicular PDL fibers (IR-PDL), and oblique PDL fibers along the root (R-PDL).

2.5. Bone Volume Fraction (BVF) of interradicular bone

Bone volume fraction (BVF) was calculated using XRM tomograms of specimens. Sub-volumes containing IR bone were isolated (Fig. 6), and bone volume fraction [38] equal to

bone volume (BV) divided by the total volume (TV) (total volume (TV) = bone volume (BV) + endosteal space) (Fig 6b) was calculated. The BV was isolated by using image segmentation (Avizo 8.1, FEI, Hillsboro, Oregon). Due to the complex geometry of the interradicular space, the total bone volume was identified by applying a morphological closing algorithm to the bone volume space, effectively including the endosteal spaces. This method was chosen over sampling cube regions in order to reduce the risk of under sampling.

3. RESULTS

3.1. Changes in biomechanical response to *in situ* loads

The biomechanics of the bone-PDL-tooth joints from respective groups was evaluated for different permutations of displacement rates and peak loads within the detectable ranges of the loading device. Load-displacement relationships (Figs. 1 and S1) were used to calculate joint stiffness by relating the displacement of the tooth within the socket to peak loads (Fig. 2a). Stiffness vs. displacement relationships revealed distinct regions based on the peak load. Higher peak loads resulted in a shift to the right shown in 2D (stiffness vs. displacement: Fig. 2a) and 3D (stiffness vs. displacement vs. age Fig. 2b and c). While both HD and SD groups demonstrated an overlap (Fig. 2b–d), fibrous joints from HD had an increased displacement response compared to SD for the same load (Fig. 2a–c).

Shifts in stiffness due to SD were plotted as a function of age and peak load with separate plots generated for different displacement rates (Fig. 2d). Mixed linear regression models identified significant shifts in stiffness (SD-HD) as a result of reduced functional loading in younger groups (8 weeks and 12 weeks) and at higher loads (peak load = 15N, disp. rate = 0.2 mm/min) (Fig. 2d). However, comparisons at older ages and at other loading schemes showed no statistical difference between diet groups (Fig. 2d).

3.2. Functional space at interradicular regions of the complex

Functional spaces using tomograms were compared between HD and SD groups across all ages (Figs. 3, S1, S2). In younger age groups (8, 12, 16 weeks), PDL functional space between and around the tooth furcation was significantly decreased in SD compared to HD group ($p < 0.05$; Student's t-test) (Fig. 3b). At older ages, functional space continued to decrease, but no statistical significance ($p > 0.05$; Student's t-test) was observed between HD and SD starting at 20 weeks of age.

3.3. Collagen fiber birefringence and root-PDL directionality in adapted complexes

Overall, oblique fibers of the root PDL (R-PDL) were well-aligned and exhibited the most birefringence under polarized light microscopy (Fig. 4c and d). Within this region, the interfaces between the PDL and bone and cementum tended to have a higher birefringence compared with regions within the PDL *per se*. The PDL near the interradicular regions of the tooth furcation were spongy in nature and showed a significant decrease in birefringence compared with R-PDL fibers (Fig. 4c). Birefringence patterns within bone revealed distinct circular patterning of birefringence around the endosteal spaces (Fig. 4c).

Birefringence intensity values of IR-PDL or bone regions did not correlate with age using our method; however the intensities increased as a function of age in both HD and SD groups within the R-PDL regions. At 8 weeks, intensities were significantly higher in HD groups compared to SD groups in R-PDL ($p<0.05$) (Fig. 4c). With an increase in age, the overall fiber angulation of the distal R-PDL decreased for both HD and SD groups (Fig. 4e).

3.4. Mechanical properties of secondary cementum, and interdental and interradicular bones

Within each specimen, the Knoop hardness of IR-bone was greater than that of interdental bone, which in turn was greater than secondary cementum (Fig. 5). Age-related trends for both HD and SD groups showed an increase in hardness for all tissues harvested from rats between 8 weeks and older. However, after 12 weeks of age, the hardness did not increase significantly with age. Tissues belonging to HD groups were harder than SD groups at 12, 16 and 24 weeks for both IR and interdental bone ($p<0.05$ two-way ANOVA/Bonferroni ad post hoc test). Cementum from HD group was harder than cementum from SD groups at 12 and 16 weeks.

3.5. Interradicular Bone Volume Fraction (BVF) as a function of age and diet

Within IR bone, bone separated from the endosteal space via segmentation is shown by comparing segmented endosteal space from IR-bone (Fig. 6a and b) and comparing identical sub-volumes of IR-bone, the apparent decrease in endosteal space (or increase in BVF) was seen (Fig. 6c). Volumetric measurements of segmented alveolar bone, showed an increase in BVF as a function of age (Fig. 6d). HD groups illustrated a significantly higher BVF compared to SD groups ($p<0.05$) at 24 weeks.

3.6. Reactionary load rates of the dentoalveolar joint

Reactionary load response patterns of the joint increased with age for both HD and SD groups (Fig. 7a). In younger groups, SD groups had a slightly increased reactionary response compared to HD groups (Fig. 7b). However, with an increase in age, reactionary response was greater in HD groups compared with SD groups (Fig. 7b).

4. DISCUSSION

The novel aspect of this study is demonstrated by mapping function-mediated adaptation of intact dentoalveolar complexes harvested from rats fed hard and soft diets respectively. The study seeks a multiscale approach, in that, stiffness of a macroscale fibrous joint and subsequently the physical properties of microscale regions within tissues that makeup the joint were evaluated and correlated.

The structural and chemical integrity of tissues is essential for joint function. In the case of a dentoalveolar fibrous joint, the cyclic chewing forces are absorbed and distributed to the surrounding tissues including the PDL, bone and cementum. The mechanically strained extracellular matrices will continue to signal cells and prompt changes in quality and architecture of respective tissues until an equilibrium is reached to meet functional demands. This is also known as functional adaptation and highlights strain-adaptive remodeling [39],

in that, the physicochemical properties of tissues that makeup the dentoalveolar joint change to accommodate functional demands. Results of this study will demonstrate this concept by 1) identifying a shift in joint stiffness due to reduced functional loads, and 2) by correlating the shift in joint biomechanics to a shift in physicochemical properties of tissues that makeup the joints exposed to reduced function. The experimental approach involved biomechanical testing of harvested joints at combinations of low to high displacement rates of low to high peaks loads using an *in situ* compression loading device. The experimental parameters to determine joint biomechanics are acceptable to identify differences in joint stiffness within and across groups, but do not mimic *in vivo* function.

The effect of reduced functional loads (SD group) on overall joint biomechanics was noted by decreased tooth displacement in the alveolar socket and was complemented by an increased joint stiffness upon compression of the tooth into the alveolar socket (Fig. 2 and S1). Since there was a relationship between the tooth displacement and joint stiffness, we turned our attention to the functional space within the dentoalveolar complex. In general, the functional space between IR bone and its respective tooth is the least when compared to any other anatomical locations [29, 31]. As such, IR bone is the first contact region, as the tooth pivots about IR bone when under function, and from a biomechanics perspective is an area where strains are predominantly concentrated [29, 31]. Given that the unopposed tooth-molar model indicated cementum accretion [40], it is conceivable that IR cementum growth due to reduced functional loads prompted an earlier contact between tooth and bone (Fig. 3, Fig. S2). However, the significant decrease in functional space as well as an increase in stiffness between the groups was only observed in the younger groups (8 and 12 weeks) with no observable changes in the older groups (16, 20, 24 weeks). Within the aforementioned argument lies a confounding factor, in that, it is plausible that the eruption rate of molars in the SD group was lower due to slower maturity of the rats. Hence rats belonging to both groups were weighed periodically (Fig. S1). No significant differences in body weights of rats were observed at earlier ages, and significant differences were observed at ages 16 weeks and older (Fig. S1). Contrasting the body weight patterns were the observed significant differences in joint stiffness at earlier ages. Hence, should the differences in joint stiffness be correlated to differences in growth rate of cementum in SD and HD groups, further scanning of the interradicular site at a higher resolution to visualize and measure cementum width is warranted.

Joint stiffness is a manifestation of shifts in adaptive physicochemical properties of bone, cementum, and the PDL. In this study, insights into the interplay between form and function at multiple length-scales were established by first coupling load response of joints harvested from SD group to tooth-bone association and subsequently to individual properties of tissues in the complex by contrasting with controls (joints harvested from HD group). The current model in dentoalveolar biomechanics is that compressive loads displace the tooth into the socket by first causing deformation in the softer ligament [29, 31]. Increased compressive loads on the tooth can cause hardening of the ligament prior to deforming mineralized tissues, primarily bone. The PDL, like many other soft tissues, from a biomechanical perspective can be modeled as a two phase system: solid and semisolid. The solid phase is composed primarily of fibrillar proteins and nonfibrillar matrix proteins, including

proteoglycans which are fundamental structural elements that interact with each other and water [41,42]. The semisolid phase of the tissue is composed of bound interstitial fluid in the PDL. The mix of the two provides the characteristic feature, that is the load response rate of the organ [29, 31]. However, joint response can continue to change due to functional adaptation of the PDL as a result of altered turnover rate of various types of collagen which can be related to respective birefringence.

The architecture of the mesial PDL is significantly different from the distal PDL. This difference is due to the presence of large vasculature predominantly at the PDL-bone enthesis, passive strain due to innate hydrostatic pressure and the electrochemical activity of the glycosaminoglycans that prompt water retention and tension within the tissue. Hence birefringence using PSR staining is specific to anatomical location within the complex and along a root. In general the architecture of IR-PDL is heterogeneous compared to the polarized architecture of the oblique fibers of R-PDL. Heterogeneous organization of the IR-PDL could explain its lower birefringence regardless of magnitude and frequency of functional loads. Relatively, the PDL fibers in mesial and distal complexes illustrated higher birefringence (Fig. 4c); a semi-quantitative marker resulting from collagen orientation, collagen quality (crosslink density) and type of collagen. Hence, the changes in intensity could be related to functional adaptation of the PDL (Fig. 4c) as a result of a change in natural turnover rate of PDL due to a change in functional load. However, a confirmatory result for functional adaptation of the PDL should be addressed using spectroscopy techniques similar to that used for cartilage degeneration [43].

The birefringence pattern in strained interradicular bone was illustrated by a circumferential pattern surrounding the endosteal spaces (Fig. 4c). Over time, it is likely that these regions will become osteons and can be termed as strain-induced adaptation underlined by circumferential collagen orientation interspersed with mineral as responsive events during remodeling [44]. These patterns increase with age as a result of increased birefringence in HD groups compared with SD groups. It is plausible that the formation of the observed birefringent rings is a response to function-mediated fluid flow over time. However, true birefringence of concentric circular or elliptical motifs (based on how the specimen was sectioned) is a challenge to measure quantitatively as polarized light is unidirectional in nature and can only capture a restricted angular range. Additional limitations include measurement sensitivity due to interfering structures within a 5–6 micron thick histology section and sectioning plane dependence of structural motifs.

Tissue structure in addition to ratio of organic to inorganic contents can affect its hardness. Rats experiencing reduced functional loads had significantly decreased hardness (Fig. 5) at older ages (12wks+) and corroborated with our previous study [20]. In particular, the hardness of IR bone was greater than interdental bone and cementum, with cementum illustrating the least hardness (Fig. 5). These shifts in mechanical properties of bone can be attributed to mechanosensitive osteocytes [45] in IR-bone.

It has long been said, that shifts in functional loads will also affect the shapes (form) of bone [46] and more recently was explained as an altered dynamics between blastic-and clasticcellular activities [47,48]. The resulting morphology can be a deviation in both the

total volume and shape of the bone as indicated by a change in bone volume fraction (BVF) (Fig. 6). Since large-scale morphological changes are evident long-term effects in tissues, BVF shifts were only statistically significant at 24 weeks (Fig. 6). Altered fluid flow due to altered functional loads could have caused a change in the number and shape of the alveoli to total bone volume. It is important to note the shift in indicators with age, that is, from joint stiffness at an earlier age to a change in tissue hardness and morphological features at a later age. Results demonstrate the capacity of form-induced strain in older animals, compared to the dominance of materialinduced differences in younger animals when compared to controls. The cumulative effect of form and material changes are better explained by illustrating a proof-of-concept on the decreased ability of joints from SD to react to simulated loads compared to HD which can react at a faster rate. Therefore, we hypothesize that softer tissues could be more sensitive to shifts in mechanical strain caused by a shift in velocity. It should be noted that the shift in kinetic energy can be a dominant factor in maintaining the needed turnover rate of the ligament to meet functional demands. The results imply a higher risk of fracture and mechanical failure in SD adapted complexes compared to HD joints for the same loads and velocities (Fig. 7).

From a biomechanics perspective, the joint stiffness and reactionary response to load altered with age. Morphometric changes within the joint space included an increase in BVF and a decrease in the joint space, resulting in a restricted tooth movement in the alveolar socket. Tissue specific changes included an increase in hardness within IR-bone, ID-bone and cementum, and an increase in collagen organization within the oblique fibers of the root PDL. These changes can be collectively seen as an adaptation to prevent joint damage when chewing harder foods. When analyzing changes due to the soft diets, the measurement of shifts in outcomes related to functional adaptation are best done by revisiting the two growth phases encapsulated within this study (rapid growth and mature stages) (Fig. 8a). Within the earlier time points when the rat is undergoing rapid growth, shifts due to the soft diet included a decrease in functional space as well a decrease in collagen organization of the root PDL. Since strain (%deformation) has been shown to be essential for tissue homeostasis, the comparative reduction of functional space may be an attempt to maintain normal physiological strain within the region (Fig. 8b and c) in response to the environmental signal. It is interesting to note that the observed growth patterns in cementum and alveolar bone are opposing, indicating differing mechanisms for mechanotransduction and/or the growth of these respective tissues (Fig. 8d). As the rat matures, shifts in joints stiffness as seen at earlier ages are not significant with age. It is suspected that the reduction in magnitude of functional loads might not be significant for continued joint adaptations albeit prompting changes in tissue architecture. Future experiments would need to be explored if a stronger stimulus (e.g. hypofunction) would produce stiffness changes in older rats. The focused timeframe of our study encapsulates observations over the period that is normally considered an active phase of laboratory rat (at and after 6 months these animals are normally retired and are minimally used for experiments).

In this study, experimental biomechanics under *ex vivo* conditions does not account for the hydrostatic pressure due to an active circulatory system [49]. However, biomechanical testing under *ex vivo* conditions can detect shifts in joint biomechanics. These shifts can be

due to form, material properties and reactionary responses of tissues to mechanical loads despite shifting the joint toward malfunction.

5. CONCLUSIONS

A reduction in functional loads resulted in short term shifts in joint biomechanics. The effects on joint stiffness are short-lived and were not observed with rapid growth and as it plateaus with age. The fact that this study showed that joint adaptation is dependent on age and that the initial form-related adaptation (observed change in functional space) can challenge tissues to meet the functional demands with increasing age well into adulthood has important clinical implications. Additionally, the coupled effect between shape and tissue properties is necessary to accommodate functional demands, and that the shifts in shape as determined by the change in functional space and bone volume fraction, and tissue properties as determined by hardness and semi-quantitative analysis of collagen birefringence are temporally sensitive despite shifting the joint to malfunction.

Supplementary Material

Refer to Web version on PubMed Central for supplementary material.

REFERENCES

1. Carter DR, Van der Meulen MCH, Beaupré GS. Mechanical factors in bone growth and development. Bone. 1996; 18:S5–S10.
2. Carter DR. Mechanical loading histories and cortical bone remodeling. Calcif. Tissue Int. 1984; 36:S19–S24. [PubMed: 6430518]
3. Ingber DE. Tensegrity: the architectural basis of cellular mechanotransduction. Annu. Rev. Physiol. 1997; 59:575–599. [PubMed: 9074778]
4. Posner AS. Crystal chemistry of bone mineral. Physiol Rev. 1969; 49:760–792. [PubMed: 4898602]
5. Dawson PE. Functional occlusion: from TMJ to smile design. Elsevier Health Sciences. 2006
6. Netter FH, Colacino S. Atlas of human anatomy. Ciba-Geigy Corporation. 1989
7. Woda A, Foster K, Mishellany A, Peyron MA. Adaptation of healthy mastication to factors pertaining to the individual or to the food. Physiol. Behav. 2006; 89:28–35. [PubMed: 16581096]
8. Kohyama K, Hatakeyama E, Sasaki T, Dan H, Azuma T, Karita K. Effects of sample hardness on human chewing force: a model study using silicone rubber. Arch. Oral Biol. 2004; 49:805–816. [PubMed: 15308425]
9. Palinkas M, Nassar MSP, Cecílio FA, Siéssere S, Semprini M, Machado-de-Sousa JP, et al. Age and gender influence on maximal bite force and masticatory muscles thickness. Arch. Oral Biol. 2010; 55:797–802. [PubMed: 20667521]
10. Waltimo A, Könönen M. A novel bite force recorder and maximal isometric bite force values for healthy young adults. Eur. J. Oral Sci. 1993; 101:171–175.
11. Grünheid T. The masticatory system under varying functional load. 2010 http://dare.uva.nl/record/328655.
12. Sako N, Okamoto K, Mori T, Yamamoto T. The hardness of food plays an important role in food selection behavior in rats. Behav. Brain Res. 2002; 133:377–382. [PubMed: 12110472]
13. Hartsfield JK, Everett ET, Al-Qawasmi RA. Genetic Factors in External Apical Root Resorption and Orthodontic Treatment. Crit. Rev. Oral Biol. Med. 2004; 15:115–122. [PubMed: 15059946]
14. Hartsfield J Jr. Pathways in external apical root resorption associated with orthodontia. Orthod. Craniofac. Res. 2009; 12:236–242. [PubMed: 19627526]
15. Nies M, Young Ro J. Bite force measurement in awake rats. Brain Res. Protoc. 2004; 12:180–185.

16. Thomas NR, Peyton SC. An electromyographic study of mastication in the freely-moving rat. Arch. Oral Biol. 1983; 28:939–945. [PubMed: 6580850]
17. Mavropoulos A, Bresin A, Kiliaridis S. Morphometric analysis of the mandible in growing rats with different masticatory functional demands: adaptation to an upper posterior bite block. Eur. J. Oral Sci. 2004; 112:259–266. [PubMed: 15154925]
18. Raadsheer MC, Kiliaridis S, Van Eijden TMGJ, Van Ginkel FC, Prahl-Andersen B. Masseter muscle thickness in growing individuals and its relation to facial morphology. Arch. Oral Biol. 1996; 41:323–332. [PubMed: 8771323]
19. Rubin CT. Skeletal strain and the functional significance of bone architecture. Calcif. Tissue Int. 1984; 36:S11–S18. [PubMed: 6430509]
20. Niver EL, Leong N, Greene J, Curtis D, Ryder MI, Ho SP. Reduced functional loads alter the physical characteristics of the bone–periodontal ligament–cementum complex. J. Periodontal Res. 2011; 46:730–741. [PubMed: 21848615]
21. Ho SP, Kurylo MP, Fong TK, Lee SSJ, Wagner HD, Ryder MI, et al. The biomechanical characteristics of the bone-periodontal ligament-cementum complex. Biomaterials. 2010; 31:6635–6646. [PubMed: 20541802]
22. Komatsu K, Chiba M. The effect of velocity of loading on the biomechanical responses of the periodontal ligament in transverse sections of the rat molar in vitro. Arch. Oral Biol. 1993; 38:369–375. [PubMed: 8328919]
23. Komatsu K, Sanctuary C, Shibata T, Shimada A, Botsis J. Stress–relaxation and microscopic dynamics of rabbit periodontal ligament. J. Biomech. 2007; 40:634–644. [PubMed: 16564051]
24. Mandel U, Dalgaard P, Viidik A. A biomechanical study of the human periodontal ligament. J. Biomech. 1986; 19:637–645. [PubMed: 3771586]
25. Ralph WJ. Tensile behaviour of the periodontal ligament. J. Periodontal Res. 1982; 17:423–426. [PubMed: 6217321]
26. Tanaka E, Inubushi T, Koolstra JH, van Eijden TM, Sano R, Takahashi K, et al. Comparison of Dynamic Shear Properties of the Porcine Molar and Incisor Periodontal Ligament. Ann. Biomed. Eng. 2006; 34:1917–1923. [PubMed: 17063388]
27. Ho SP, Kurylo MP, Grandfield K, Hurng J, Herber R-P, Ryder MI, et al. The plastic nature of the human bone–periodontal ligament–tooth fibrous joint. Bone. 2013; 57:455–467. [PubMed: 24063947]
28. Jang AT, Lin JD, Seo Y, Etchin S, Merkle A, Fahey K, et al. In situ Compressive Loading and Correlative Noninvasive Imaging of the Bone-periodontal Ligament-tooth Fibrous Joint. J. Vis. Exp. 2014
29. Lin JD, Özcoban H, Greene JP, Jang AT, Djomehri SI, Fahey KP, et al. Biomechanics of a bone–periodontal ligament–tooth fibrous joint. J. Biomech. 2013; 46:443–449. [PubMed: 23219279]
30. Naveh GRS, Shahar R, Brumfeld V, Weiner S. Tooth movements are guided by specific contact areas between the tooth root and the jaw bone: A dynamic 3D microCT study of the rat molar. J. Struct. Biol. 2012; 177:477–483. [PubMed: 22138090]
31. Lin JD, Lee J, Özcoban H, Schneider GA, Ho SP. Biomechanical adaptation of the bone-periodontal ligament (PDL)-tooth fibrous joint as a consequence of disease. J. Biomech. 2014; 47:2102–2114. [PubMed: 24332618]
32. Chiba M, Komatsu K. Mechanical responses of the periodontal ligament in the transverse section of the rat mandibular incisor at various velocities of loading in vitro. J. Biomech. 1993; 26:561–570. [PubMed: 8478357]
33. Fung, YC. Biomechanical Aspects of Growth and Tissue Engineering. Springer New York: Biomechanics; 1990. p. 499-546.http://link.springer.com/chapter/10.1007/978-1-4419-6856-2_13 [accessed January 9, 2015]
34. Popowics T, Yeh K, Rafferty K, Herring S. Functional cues in the development of osseous tooth support in the pig, Sus scrofa. J. Biomech. 2009; 42:1961–1966. [PubMed: 19501361]
35. Ho SP, Balooch M, Marshall SJ, Marshall GW. Local properties of a functionally graded interphase between cementum and dentin. J. Biomed. Mater. Res. A. 2004; 70A:480–489. [PubMed: 15293322]

36. ASTM - E04 Committee, Test Method for Microindentation Hardness of Materials. ASTM International. 1999 http://enterprise.astm.org/filtrexx40.cgi?HISTORICAL/E384-99.htm.
37. Fiji Is Just ImageJ, (n.d.). http://fiji.sc/wiki/index.php/Fiji.
38. Parfitt AM. Bone histomorphometry: Proposed system for standardization of nomenclature, symbols, and units. Calcif. Tissue Int. 1988; 42:284–286. [PubMed: 3135094]
39. Prendergast PJ, Taylor D. Prediction of bone adaptation using damage accumulation. J. Biomech. 1994; 27:1067–1076. [PubMed: 8089161]
40. Murphy T. Compensatory mechanisms in facial height adjustment to functional tooth attrition. Aust. Dent. J. 1959; 4:312–323.
41. Nanci A. Ten Cate's Oral Histology-Pageburst on VitalSource: Development, Structure, and Function. Elsevier Health Sciences. 2007
42. Ho SP, Sulyanto RM, Marshall SJ, Marshall GW. The cementum–dentin junction also contains glycosaminoglycans and collagen fibrils. J. Struct. Biol. 2005; 151:69–78. [PubMed: 15964205]
43. Boskey A, Camacho NP. FT-IR imaging of native and tissue-engineering bone and cartilage. Biomaterials. 2007; 28(15):2465–2478. [PubMed: 17175021]
44. Bromage TG, Goldman HM, McFarlin SC, Warshaw J, Boyde A, Riggs CM. Circularly polarized light standards for investigations of collagen fiber orientation in bone. Anat. Rec. B. New Anat. 2003; 274B:157–168. [PubMed: 12964206]
45. Qing H, Bonewald LF. Osteocyte Remodeling of the Perilacunar and Pericanalicular Matrix. Int. J. Oral Sci. 2009; 1:59–65. [PubMed: 20687297]
46. Wolff, J. Das Gesetz der Transformation der knochen. Berlin: A. Hirschwald; 1892. (This monograph was translated to English and was published by Springer-Verlag in 1986).
47. Frost HM. Bone "mass" and the" mechanostat": A proposal. Anat. Rec. 1987; 219:1–9. [PubMed: 3688455]
48. Frost HM. Bone's mechanostat: A 2003 update, Anat. Rec. A. Discov. Mol. Cell. Evol. Biol. 2003; 275A:1081–1101.
49. McCauley, LK.; Somerman, MJ. Mineralized Tissues in Oral and Craniofacial Science: Biological Principles and Clinical Correlates. John Wiley & Sons; 2012.

HIGHLIGHTS

- Organ-level function-mediated changes are linked to morphology at a younger age and subsequently to physicochemical properties of tissues.
- Biophysical and biochemical adaptations in bone and PDL could be similar, but could inversely affect cementum to meet functional demands.
- Functional adaptation of bone, cementum, and the periodontal ligament are dependent on age.
- Adaptations are registered as functional history in tissues and joints.

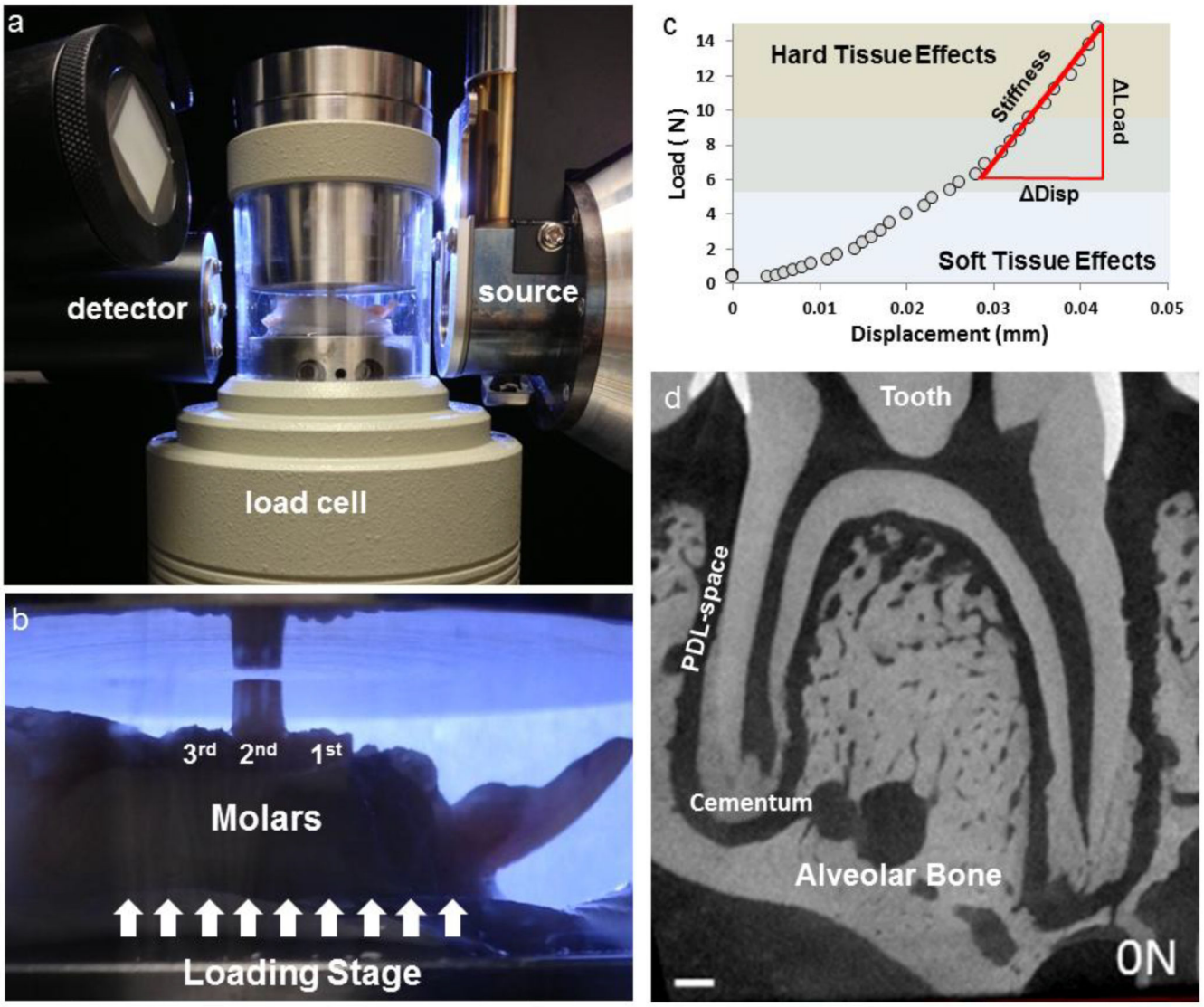

Figure 1. *In situ* loading device coupled to a XRM system to image tooth motion relative to the alveolar socket

a) Hemimandibles were prepared with composite buildups for mechanical testing and were placed in the load cell as shown. b) To ensure a parallel surface between the anvil and the composite buildup, occlusal marking paper was used (not shown) to mark uniform area of contact. c) The output of load displacement curve was analyzed by comparing the change in load (Δ Load) vs. the change in displacement (Δ Disp). d) 2D virtual section relating tooth to the alveolar socket. Please note that 1d is a GIF file and should be viewed under slide show.

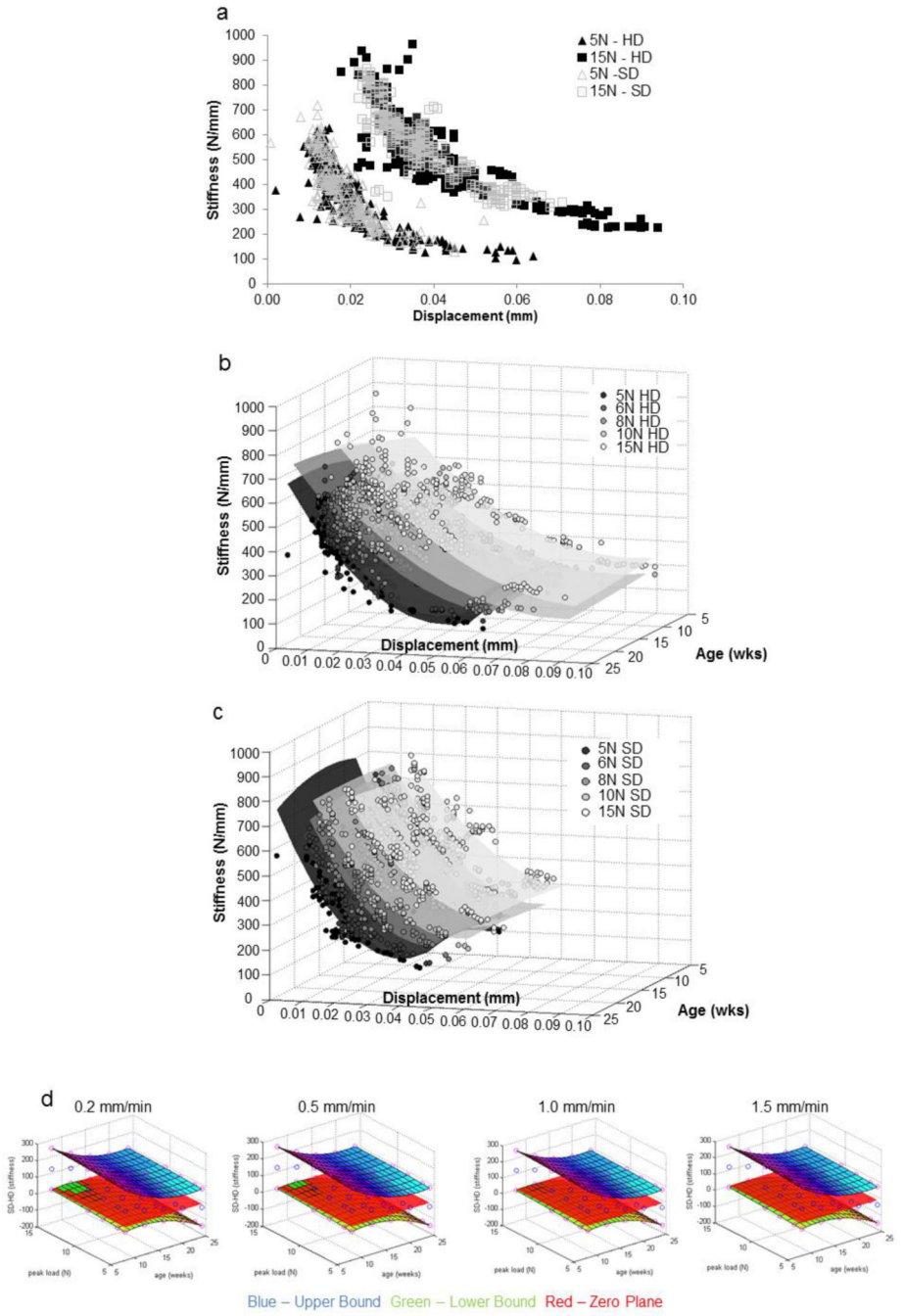

Figure 2. Stiffness values for fibrous joints obtained from those fed hard and soft diets respectively

a) The nonlinear plot illustrate joint stiffness values from all age groups when individually tested at different speeds (0.2, 0.5, 1.0, 1.5, 2.0 mm/min) and when loaded to 5 N (triangles – open and filled) and 15 N (squares – open and filled) respectively. Data for 6, 8, and 10 N are not shown but showed similar trends. The graph illustrates an increased range in displacement of the teeth from the HD group compared to displacement of teeth from SD group. 3D surface plots illustrate different spread of stiffness values with age (wks) and displacement (mm) when tested for peak loads of 5, 6, 8, 10, and 15 N in (b) HD groups and

(c) SD groups. d) Statistical differences between stiffness values calculated from load-displacement relationships were analyzed using a mixed effects regression model and plotted as a function of age of the mammal. From the resulting 95% confidence intervals (blue – upper bound, green – lower bound, red – zero plane) the notable difference is that the joints from younger animals (8 and 12 week) in soft diet group were significantly stiffer than the joints from hard diet group under hard diet load-simulation conditions (higher load, lower displacement rate).

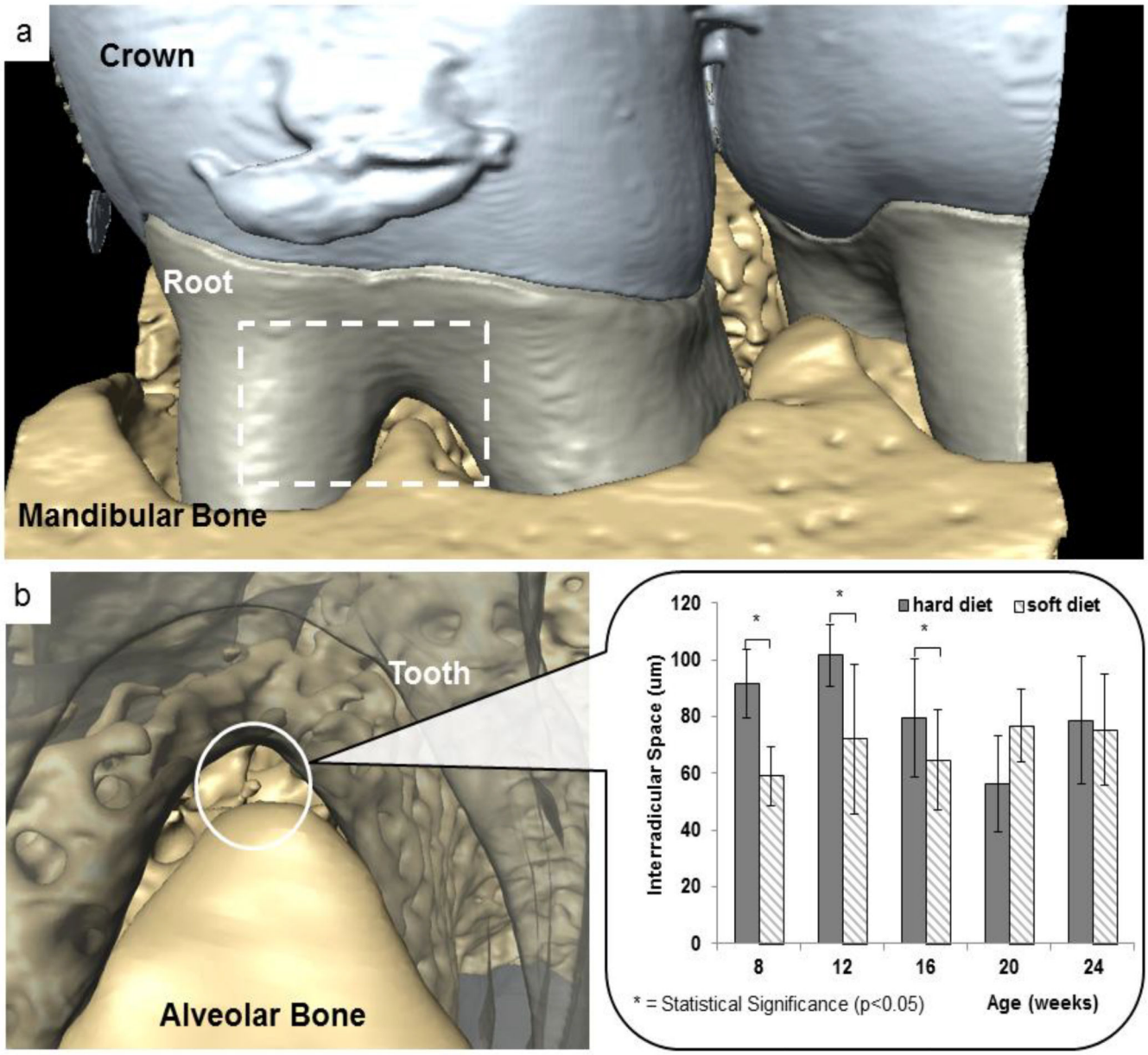

Figure 3. XRM tomography measurements of interradicular PDL-space

a) Representative tomogram illustrating a bone--PDL-tooth complex. Functional space was measured within the interradicular region (white dotted box). b) At younger groups, a narrower interradicular space was observed in soft diet groups compared with hard diet groups. However, with an increase in age, the difference between hard and soft diet groups became less significant.

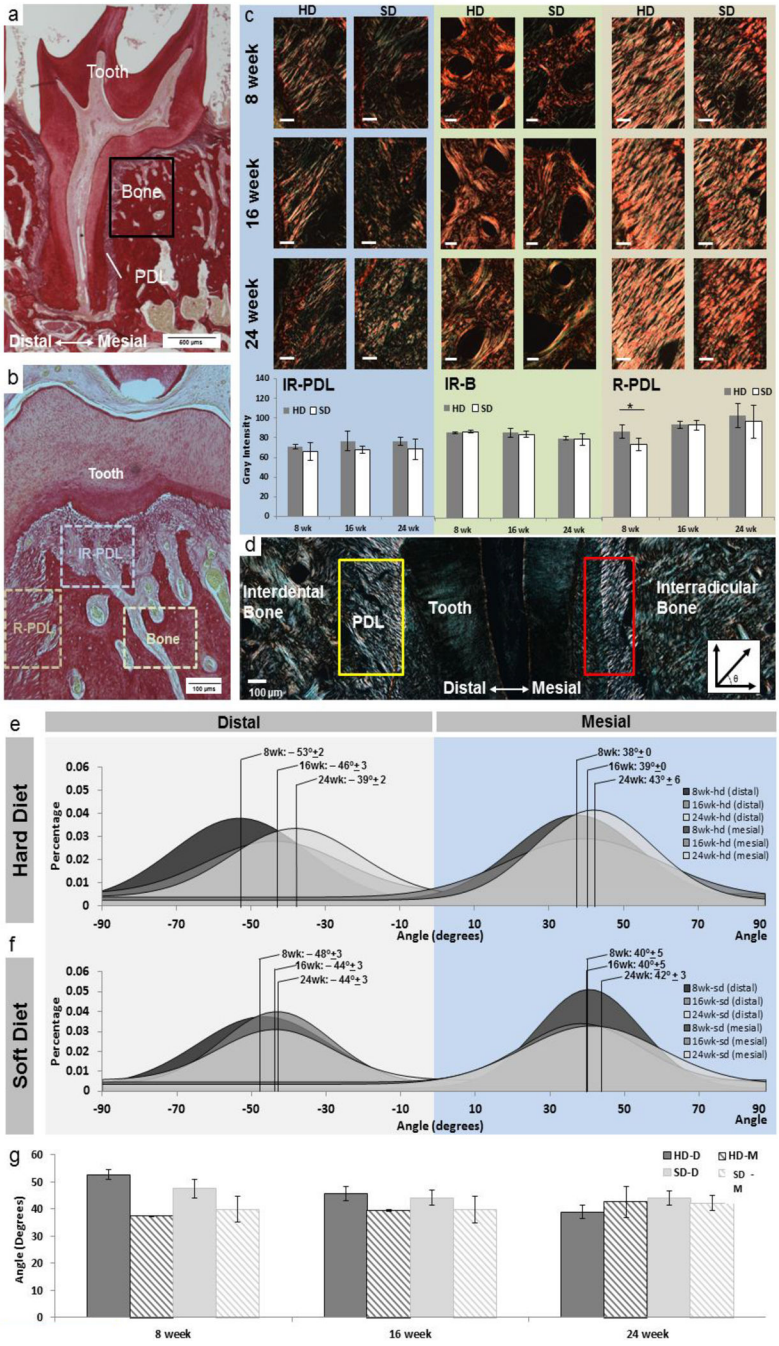

Figure 4. Collagen birefringence and PDL directionality across groups and age

a) Histology sections were stained with picrosirius red. b) Imaging was primarily focused around the furcation and root-PDL (R-PDL) surrounding the distal root of the 2nd molar. c) Birefringence signal was measured in the following regions: interradicular bone (IR-B), interradicular periodontal ligament (IR-PDL), and R-PDL. IR-PDL revealed a sponge-like configuration while R-PDL illustrated an increased collagen fiber orientation. Under polarized light, collagen orientation was quantified within IR-PDL, IR-B, and R-PDL. White bars are 100 μms. Trends show increased birefringence as a function of age within PDL

regions and a decrease in birefringence as a function of age within interradicular bone. Statistical significance in birefringence between SD and HD is indicated with an (*) ($p<0.05$) and was only observed in the PDL of 8 week old. Graphical representation of averages and standard deviations show no age-related trends for both hard and soft diet groups. (d) Images using polarized light microscopy show regions of distal (yellow box) and mesial (red box) regions used to calculate fiber orientation. Representative histogram distributions of fiber orientation in (e) hard diet and (f) soft diet are shown for 8, 16, and 24 weeks with total group average and standard deviations are shown. g) As a function of age trends included a decreasing difference in distal- and mesial-PDL orientation within and across hard and soft diet groups with age.

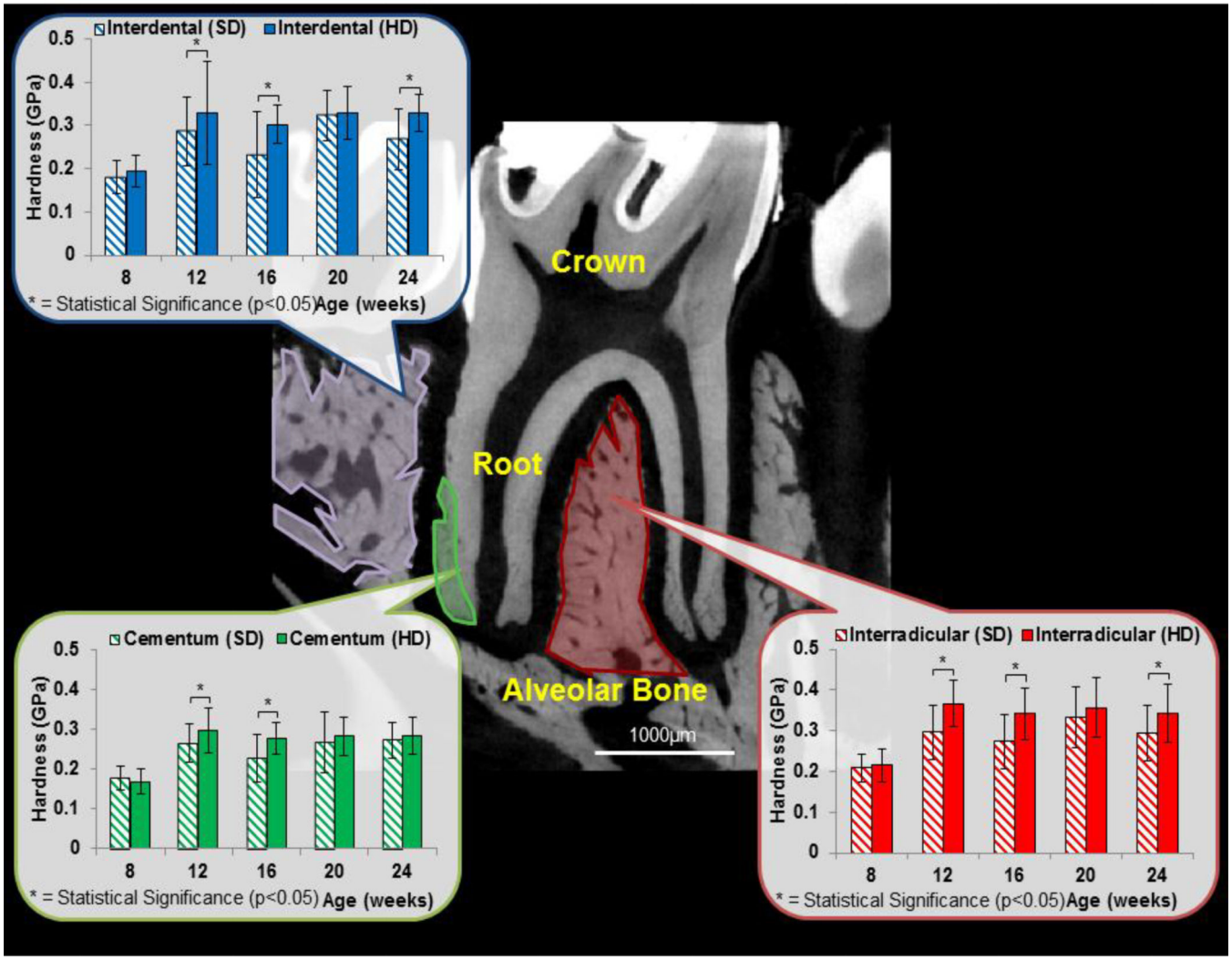

Figure 5. Microindentation and interradicular functional space of bone-PDL-tooth complexes

Microindentation was performed on cementum, interdental bone and interradicular bone. In general, interradicular bone was always harder than interdental bone which was always harder than cementum. While age-related trends were not found, hard diet groups illustrated an increased interradicular bone hardness compared to bone from rats on a softer diet. Additionally, interradicular functional space was measured by taking standard virtual sections between the distal and mesial buccal roots. Results show that interradicular space decreased in younger rats fed softer diet. *indicates statistical significant difference ($p<0.05$).

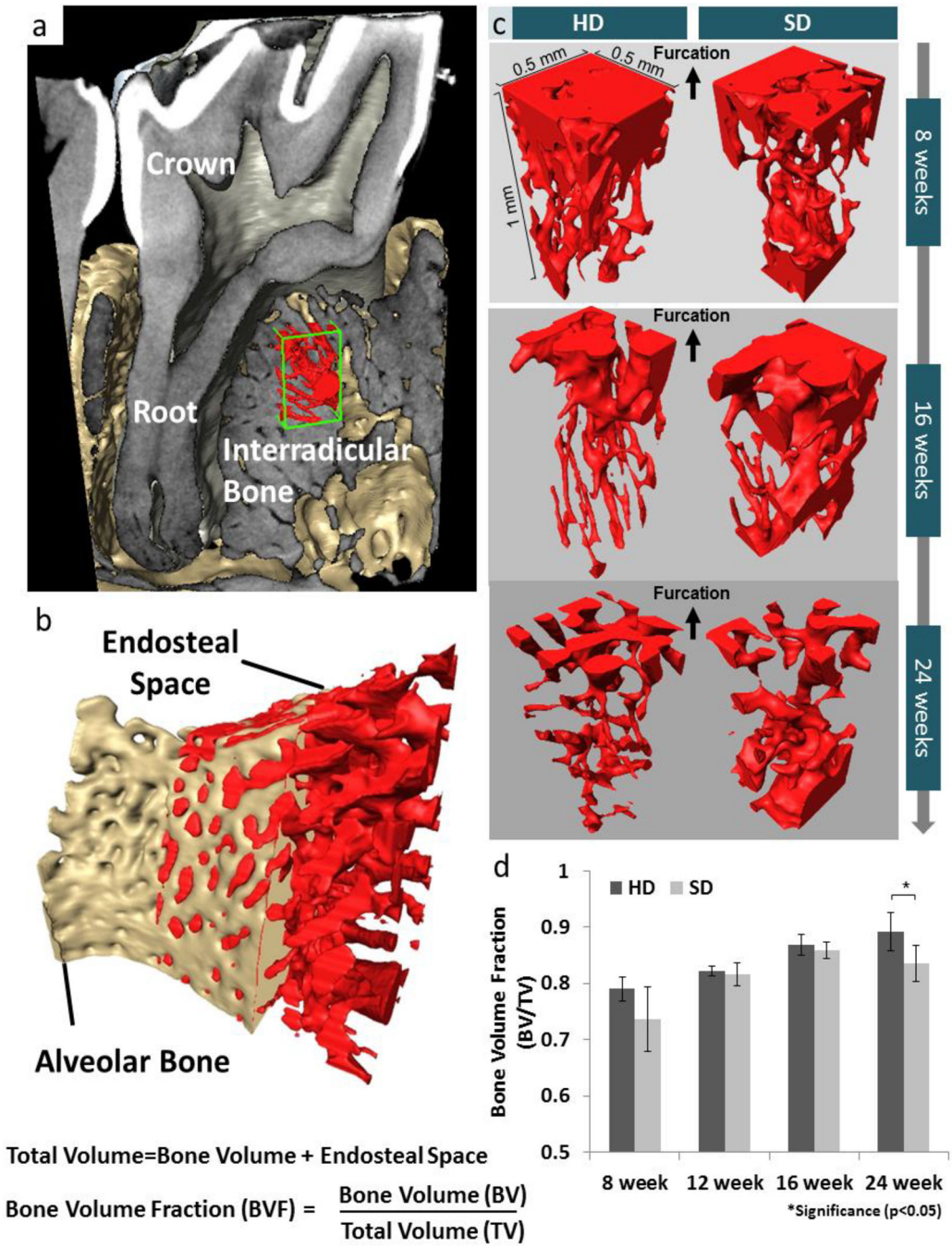

Figure 6. Comparison of bone volume fraction (BVF) of interradicular alveolar bone by using XRM tomography

(a) Digitally reconstructed structure of tooth in the alveolar socket illustrate the volume of interest in alveolar bone. (b) Bone volume fraction is illustrated as the ratio between bone volume to total volume (bone volume + endosteal volume (c)). (c) Endosteal volume decreased with age in both groups. However, greater endosteal volume in interradicular bone from those fed softer diet were observed. (d) BVF of HD was significantly higher than that of SD at 24 weeks.

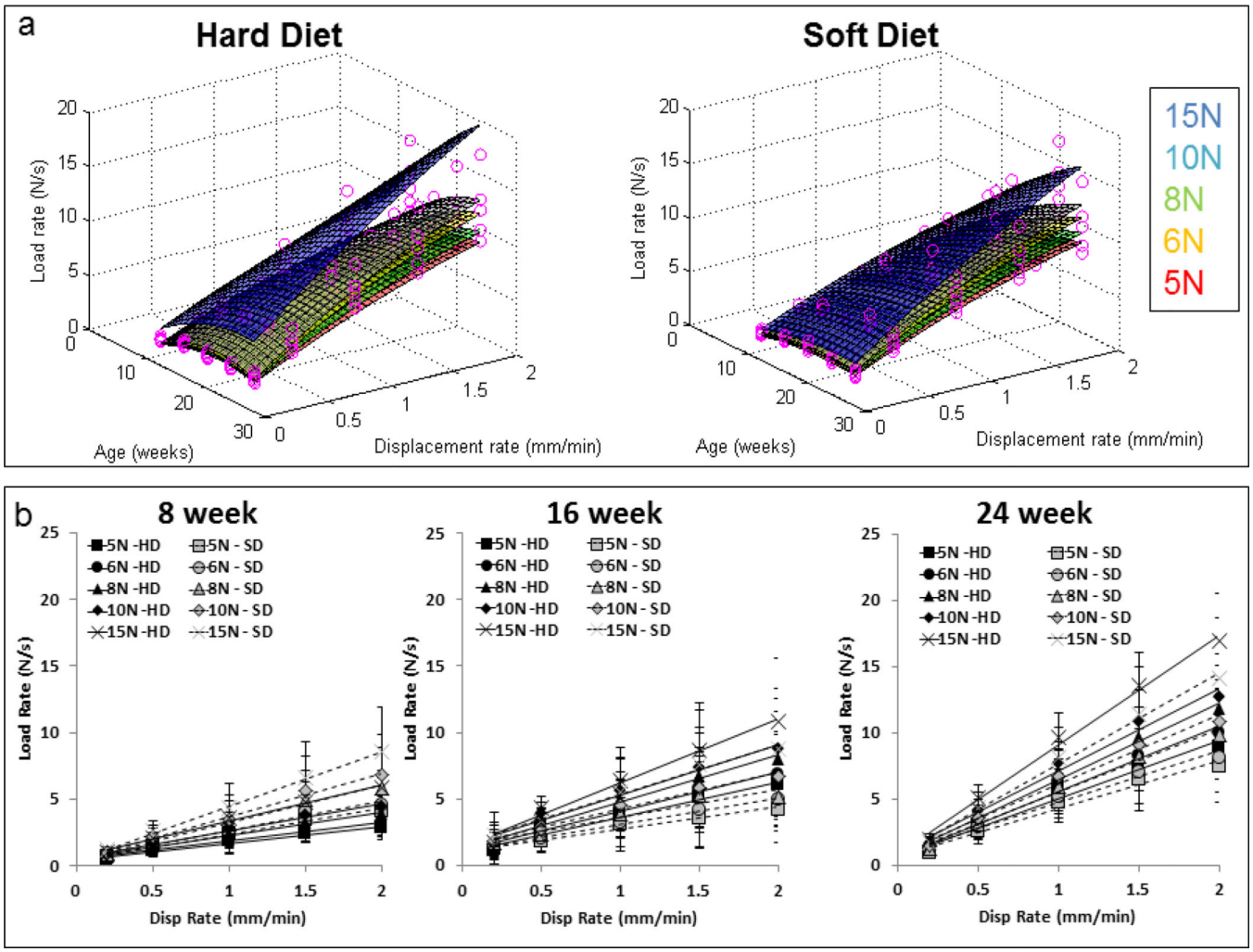

Figure 7. Comparison of reactionary responses of joints to loads

a) Higher reactionary response to load for HD older group was observed. b) Although similar trends were seen to a certain extent, the obvious trend was that the younger group fed SD demonstrated a higher reactionary response compared to its HD counterpart. Similar trend was not observed with an increase in age.

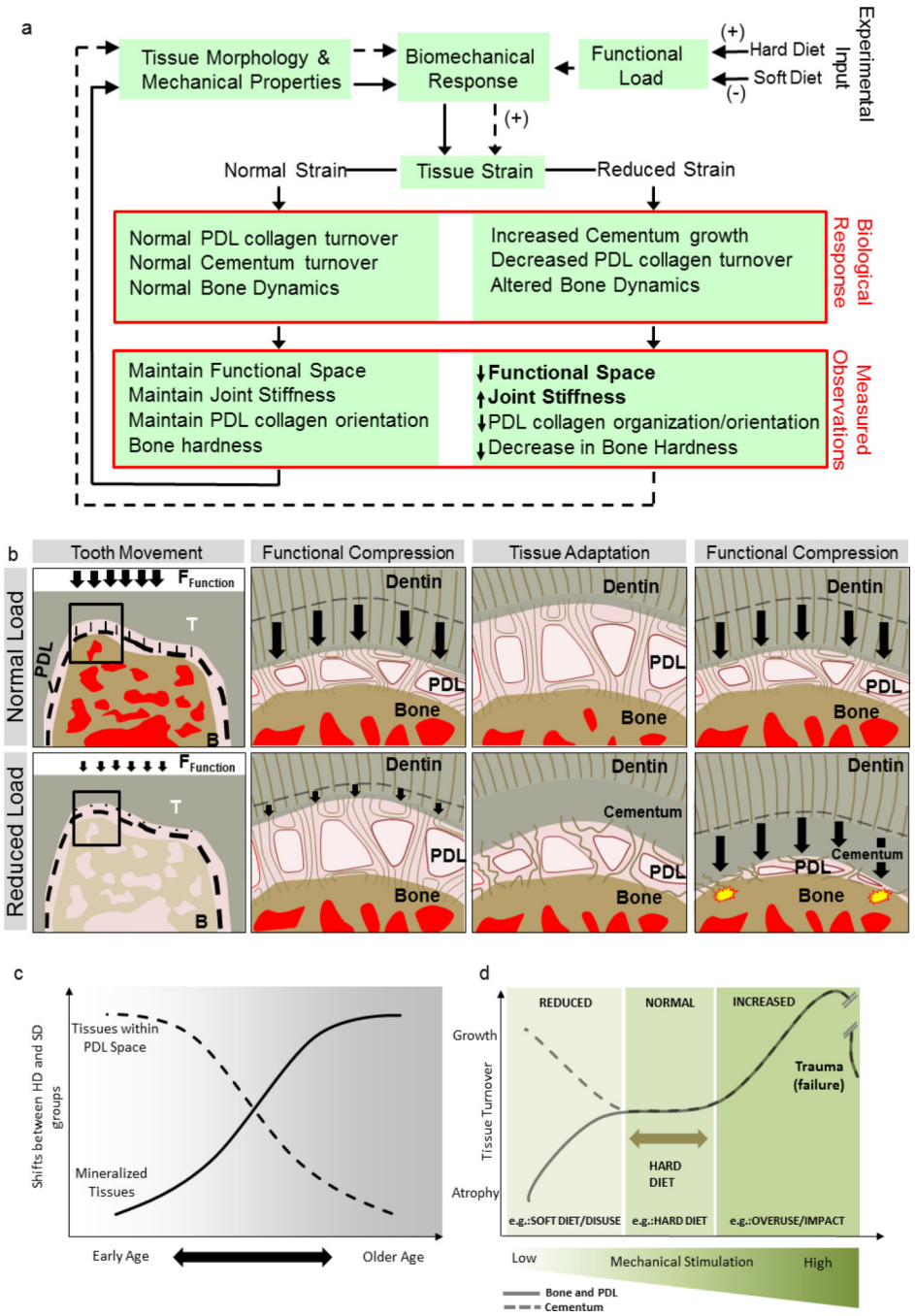

Figure 8. Postulated load-mediated adaptation of the dentoalveolar complex

a) Experimental workflow showing different food consistencies given to control (HD) and SD groups and changes in observed biological responses. (b) The fibrous joint compensates through decreased PDL-space through ingrowth of cementum and decreased orientation and organization of the collagen fibers. The shift in input signal prompts a shift in adaptive properties of tissues as indicated by site-specific measurements. However, if normal functional loads are placed on adapted tissues belonging to the SD diet group, they would likely be seen as traumatic loads prompting a damage response (yellow start bursts). (c)

Shifts in outcomes due to load-mediated adaptations can be divided into two phases; early ages focused around the tissues within the PDL space, and shifts seen at later ages primarily as changes in bone mineral content and internal structure. (d) Normally chewing loads are accommodated by the dentoalveolar complex through compression of supporting tissues (PDL, bone, cementum) causing physiological strain due to tissue deformation (mixed-mode) and fluid flow from interstitial fluid movement. Mechano-responsiveness of localized cells in the regions of higher fluid flux and mechanical strain regulate a shift in tissue turnover in bone and the PDL morphology and material properties accordingly. A reduction of functional loads net a decrease in strain and is felt by the supporting tissue away from the physiological strain. Within bone, atrophy of tissue is usually seen, however, the opposite effect (growth) has been reported within cementum tissues.